Unmasking silent endothelial activation in the cardiovascular system using molecular magnetic resonance imaging.

Julie Belliere, Sara Martinez de Lizarrondo, Robin P. Choudhury, Aurélien Quenault, Audrey Le Béhot, Christine Delage, Dominique Chauveau, Joost P. Schanstra, Jean-Loup Bascands, Denis Vivien, Maxime Gauberti.

SUPPLEMENTARY INFORMATION

Supplementary Figure 1. Sonication disperses particle aggregates and avoids unspecific plugging of brain vessels.

Supplementary Figure 2: Semi-automatic threshold for MPIO-induced signal void.

Supplementary Figure 3: LPS induces VCAM-1 overexpression in the kidney, brain and heart vascular beds.

Supplementary Figure 4: Longitudinal fast T2*-weighted imaging of the kidneys and the inferior vena cava of LPS-treated mice, after intravenous injection of MPIO-αVCAM-1.

Supplementary Figure 5: Longitudinal fast T2*-weighted imaging of the brain of LPS-treated mice before and after intravenous injection of MPIO-αVCAM-1.

Supplementary Figure 6: non-specific MPIO uptake by the liver and the spleen**.**

Supplementary Figure 7: Creatininemia and blood urea nitrogen (BUN) plasmatic levels in control (saline) and glycerol-treated mice 48 hours and 8 days after treatment.

Supplementary Figure 8: Rhabdomyolysis induced endothelial activation in the kidneys.

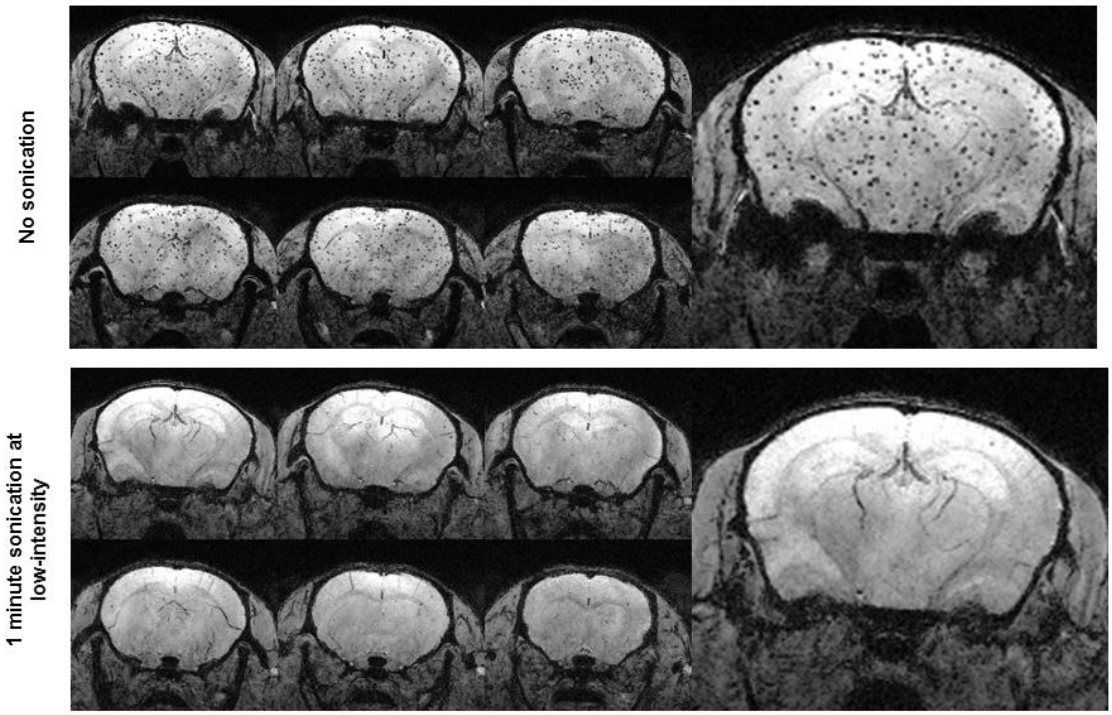

Supplementary Figure 1. Sonication disperses particle aggregates and avoids unspecific plugging of brain vessels. MPIO aggregates are visible as small black dots and are no more present after sonication of the solution before intravenous administration. MRI acquisition was performed as described in the material and methods section.

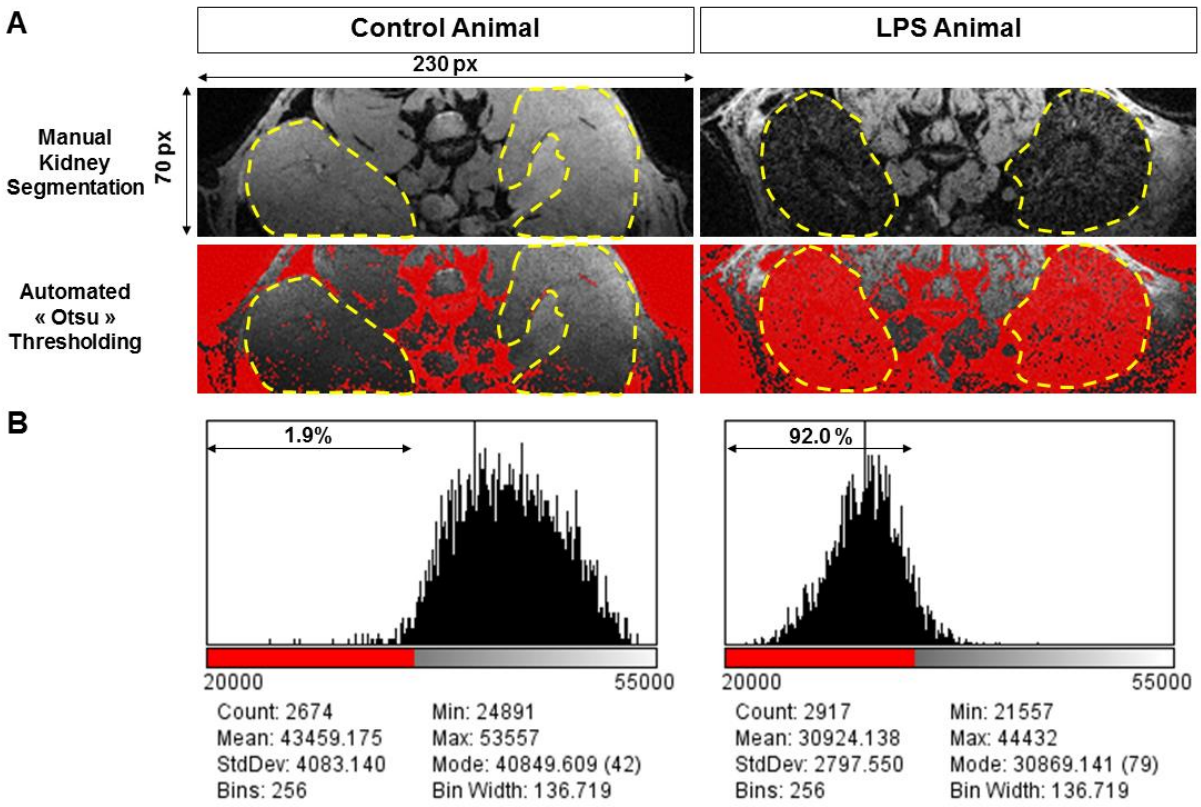

Supplementary Figure 2. Semi-automatic threshold for MPIO-induced signal void. (A) Representative T2*-weighted images of the kidneys from a control and a LPS-treated animal after MPIO-αVCAM-1 injection. The first step is to crop the initial MRI in a 230x70 pixels picture, including both kidneys. Then, the kidneys are manually segmented (delimitated by dotted yellow lines, excluding the pyelocalicial cavities). Lastly, 3D Otsu automated threshold is applied using ImageJ software and the signal void volume is computed (in percentage of the total kidney volume). (B) Results of the thresholding procedure.

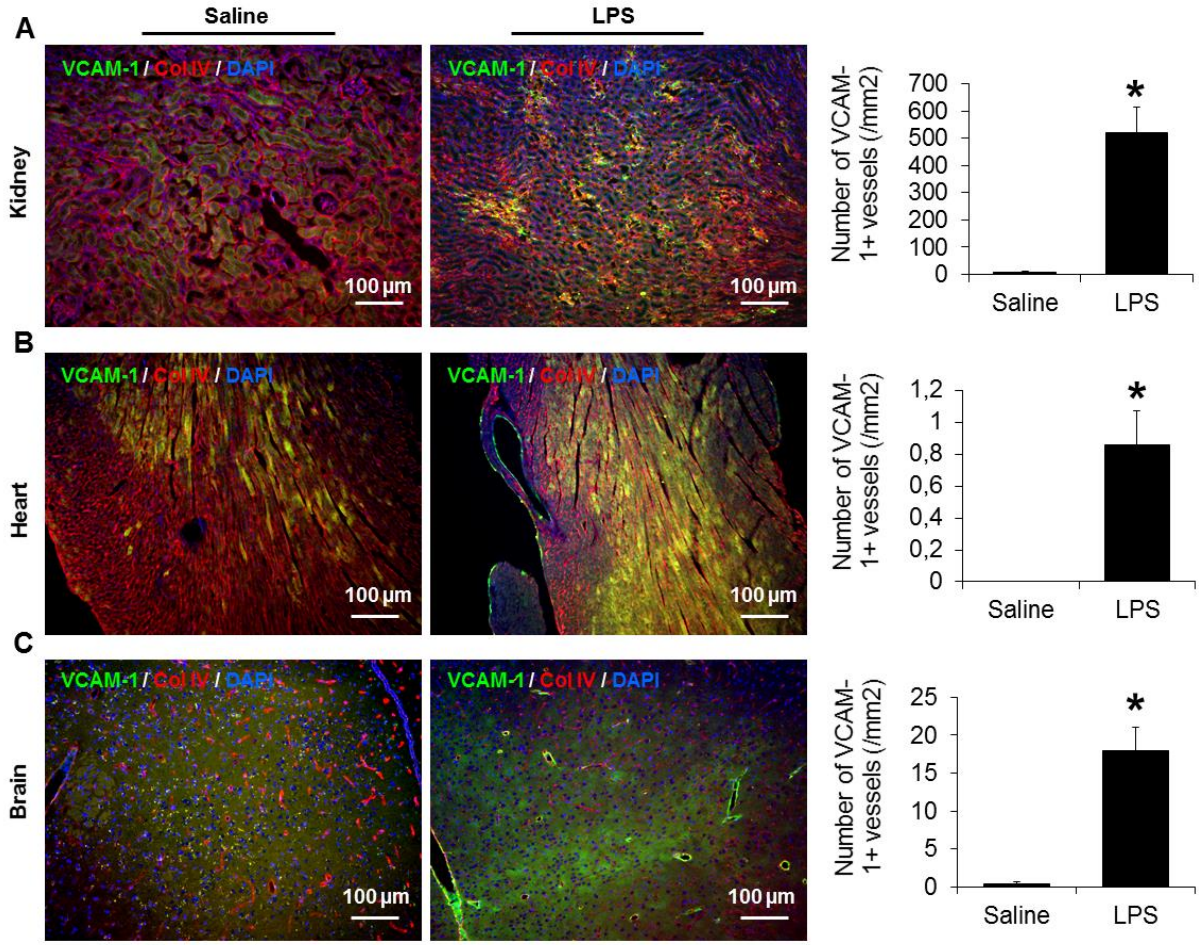

Supplementary Figure 3. LPS induces VCAM-1 overexpression in the kidney, brain and heart vascular beds. (A) Left: Representative immunohistological images of VCAM-1 expression (green) in the kidneys of control (saline) and LPS-treated mice (1 mg/kg, 48 hours after i.p. injection). Right: Corresponding quantification. (B) Same as in A, but for the heart. Since auto-fluorescence prevents reliable analysis of VCAM-1^{+} vessels in the cardiac microcirculation, only large vessels (>20 µm) were considered in the analysis. (C) Same as in A, but for the brain. Collagen type IV (Col IV, Red) and DAPI (Blue) were used to assess tissue morphology. All conditions were performed n=3/group. *p<0.05 vs control (saline).

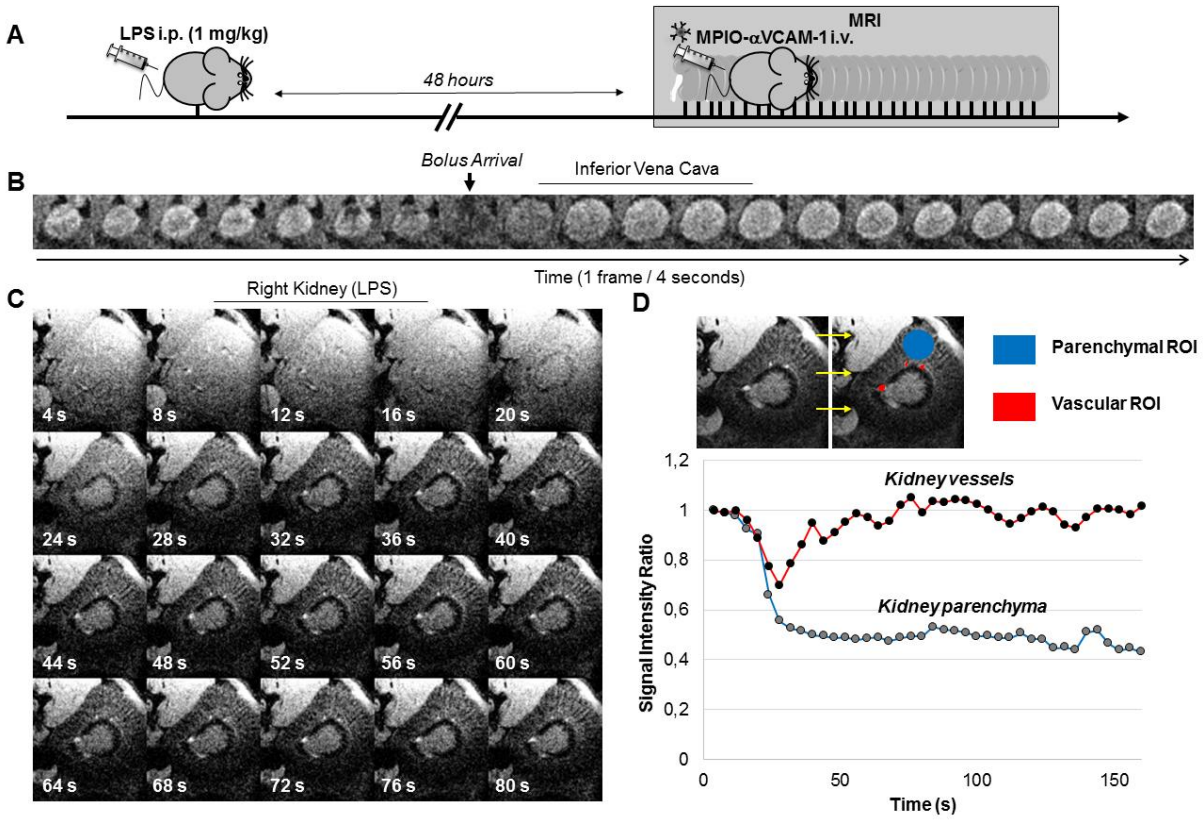

Supplementary Figure 4. Longitudinal fast T2*-weighted imaging of the kidneys and the inferior vena cava of LPS-treated mice, after intravenous injection of MPIO-αVCAM-1. The experiments presented in this figure were performed 3 times to ensure reproducibility. (A) Experimental design. (B) Representative T2*-weighted images of the inferior vena cava after intravenous injection of MPIO-αVCAM-1, revealing vascular signal drop during MPIO injection (indicated by the black arrow) but complete recovery immediately thereafter. (C) Representative T2*-weighted images of the right kidney after intravenous injection of MPIO-αVCAM-1, revealing persistent signal void in the kidney parenchyma after the first pass of the contrast-agent. No further contrast enhancement is seen after the first pass, which is in accordance with the very short half-life of plasmatic MPIO. (D) Quantification of the signal changes in the animals presented in (C), with a representative image. Parenchyma and vascular areas are indicated in blue and red respectively. Large kidney vessels were easily identified in the post-contrast images. The parenchymal ROI was chosen as close as possible from the magnet receiving coil to improve signal to noise ratio. ROI = Region of interest, s= seconds.

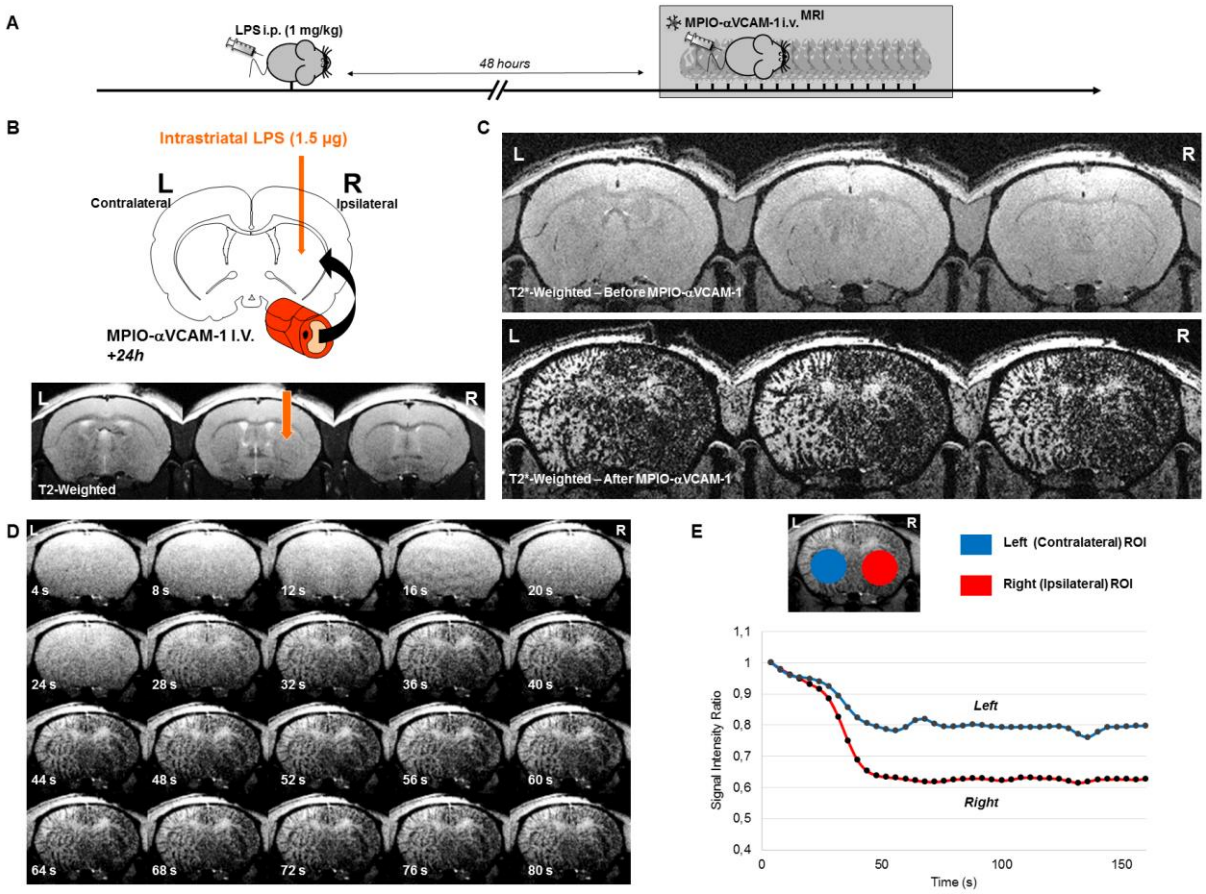

Supplementary Figure 5. Longitudinal fast T2*-weighted imaging of the brain of LPS-treated mice before and after intravenous injection of MPIO-αVCAM-1. The experiment presented in this figure was performed 3 times to ensure reproducibility. (A) Experimental design. (B) Mice received an intra-striatal injection of 1.5 µg of LPS in the right (R) striatum. (C) Representative consecutive slices from T2*-weighted images of the brain before and after intravenous injection of MPIO-αVCAM-1, revealing intense inflammation predominating in the ipsilateral (R, right) striatum as compared to the contralateral one (Left, L). (D) Representative fast T2*-weighted images of the brain after intravenous injection of MPIO-αVCAM-1, revealing persistent signal void in the brain (predominating in the right side) after the first pass of the contrast-agent. No further contrast enhancement is seen after the first pass, which is in accordance with the very short half-life of plasmatic MPIO-αVCAM-1. (E) Quantification of the signal changes in the animal presented in (D), with a representative image. Left and right striatal areas are indicated in blue and red respectively. ROI = Region of interest, s= seconds.

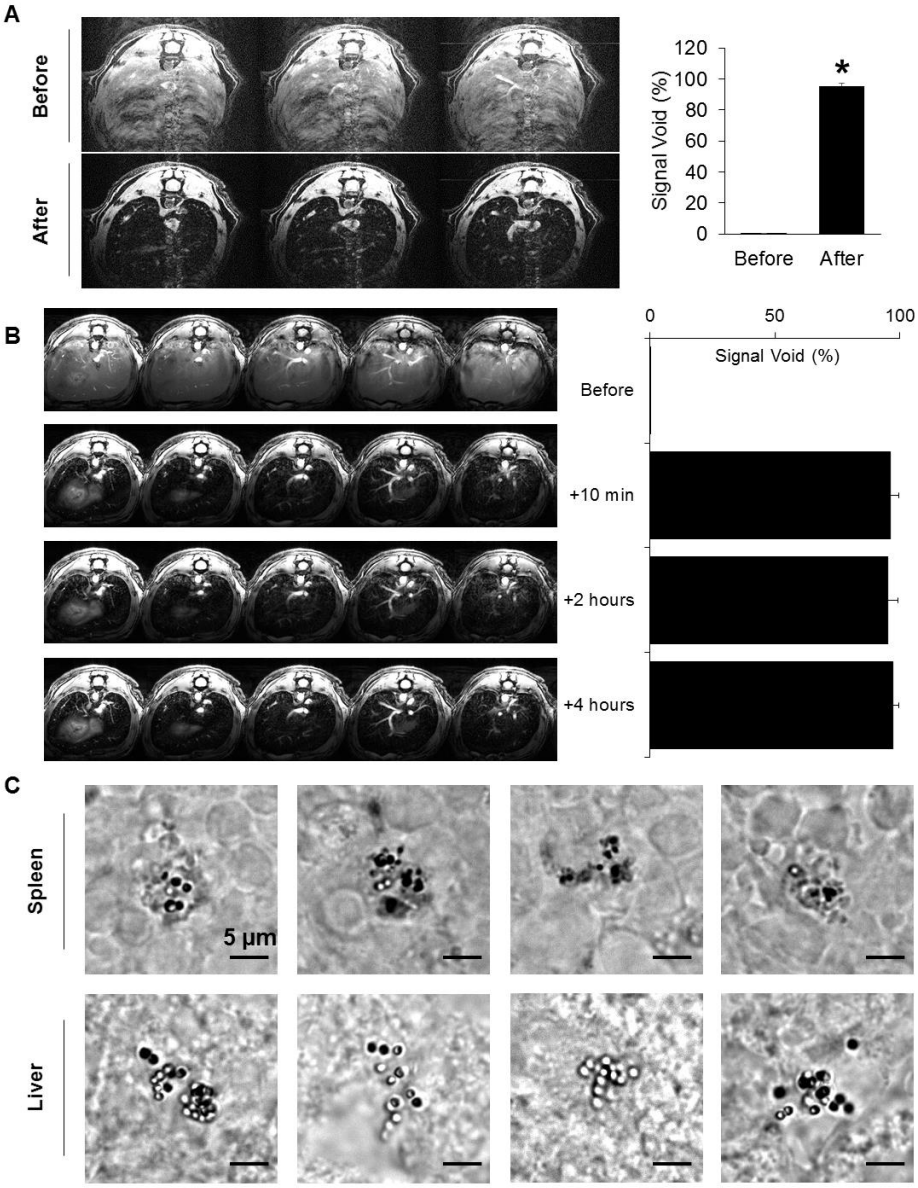

Supplementary Figure 6: non-specific MPIO uptake by the reticulo-endothelial system. (A) Left: Representative high-resolution T2*-weighted images before and 10 minutes after administration of MPIO-αVCAM-1 in a control mouse, revealing significant uptake in the liver and the spleen (not shown). Right: Corresponding quantification (only data concerning the liver are represented, n=3). (B) Left: Representative T2*-weighted images of the liver (using "intragate" to avoid movement artifacts) acquired before, 10 minutes, 2 hours and 4 hours after MPIO-αVCAM-1 administration, showing rapidly appearing and persistent hyposignal in the liver. Right: Corresponding quantification (n=3). (C) Representative histological images of the spleen and liver showing numerous MPIO-αVCAM-1 sequestrated in both organs. MPIOs were present in clusters suggesting intracellular distribution inside macrophages of the reticulo-endothelial system.

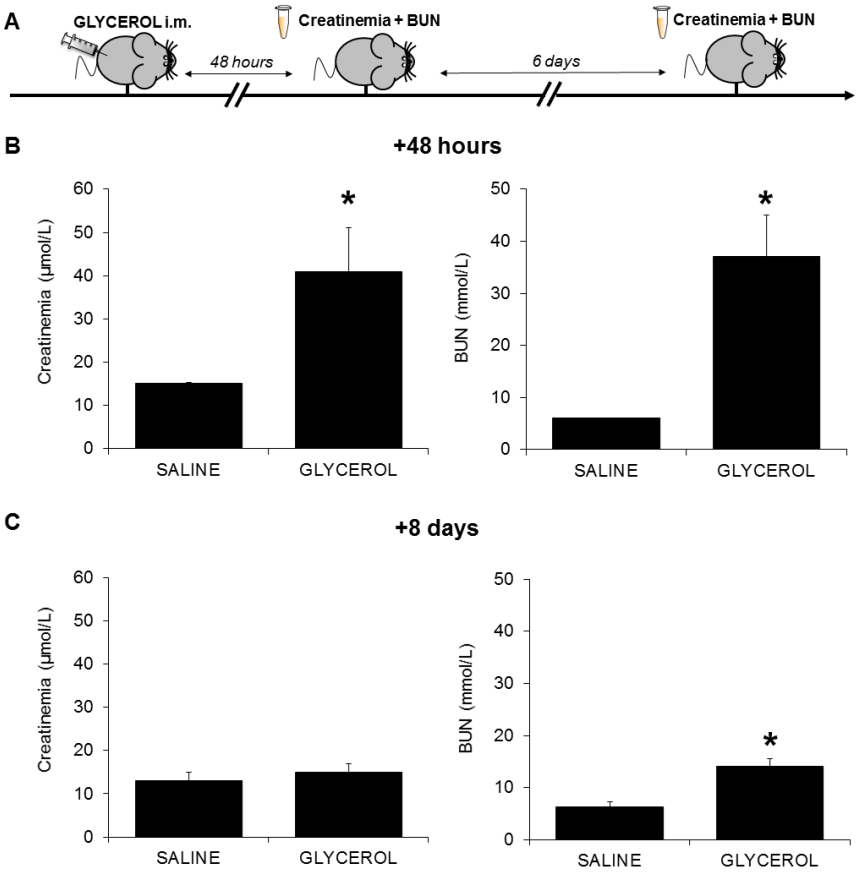

Supplementary Figure 7. Creatininemia and blood urea nitrogen (BUN) plasmatic levels in control (saline) and glycerol-treated mice 48 hours and 8 days after treatment. (A) Experimental design. (B) 48 hours or (C) 8 days after glycerol or saline injection (n=5/group). Dosages were performed using ELISA. *p<0.05 vs control (saline).

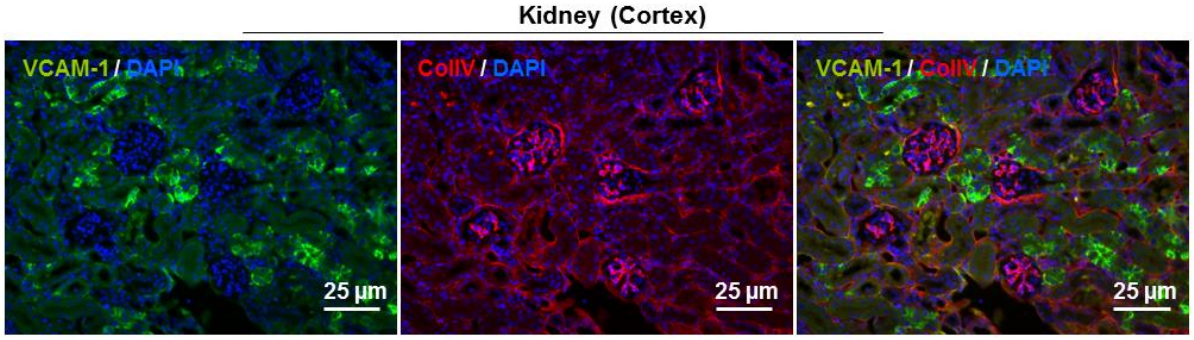

Supplementary Figure 8. Rhabdomyolysis induced endothelial activation in the kidneys. Representative immunohistological images of the kidney (cortex) 2 days after glycerol treatment. VCAM-1 overexpression (presented in green) in glycerol-treated mice is extra-glomerular. Collagen type IV (Col IV, in red) and DAPI (in Blue) were used to assess renal tissue morphology.